International Journal of Adhesion and Adhesives 84 (2018) 368–377

Contents lists available at ScienceDirect

International Journal of Adhesion and Adhesives

journal homepage: www.elsevier.com/locate/ijadhadh

Failure mechanism of glass-fiber reinforced laminates influenced by the copper film in three-point bending

Pengliang Hou[a], Anran Zhao[a], Weidong Wu[a], Haixiang Huan[a], Cong Li[b], Shunbo Wang[b], Hongwei Zhao[b,*]

[a] School of Mechanical Engineering, Yancheng Institute of Technology, Yancheng 224051, China
[b] School of Mechanical Science and Engineering, Jilin University, Changchun 130025, China

ARTICLE INFO

Keywords:
Glass-fiber
Copper-clad laminates
In situ
Finite element analysis
Acoustic emission

ABSTRACT

In this paper the influence of copper film on the stress distribution, damage evolution and failure mechanism of glass-fiber reinforced laminates was investigated. The specimens were tested at the *in situ* three-point bending tester. Simultaneously, a microscope and acoustic emission (AE) system were applied to *in situ* characterize the damage evolution of surface and inside of specimens, respectively. Moreover, a finite element analysis (FEA) model was constructed to simulate the stress distribution on the different types of specimens during the three-point bending. The result of the finite element simulation was in agreement with that of the experiment. The bending stress distribution on the specimen of glass-fiber reinforced laminates (no copper film) and double-sided copper-clad laminates was different from that of the single-sided copper-clad laminates, which made the failure mechanism of single-sided copper-clad laminates was not the same as the glass-fiber reinforced laminates and double-sided copper-clad laminates. It is obviously that the copper film can effectively improve the mechanical properties of glass-fiber reinforced laminates. The *in situ* images revealed the damage evolution of glass-fiber reinforced laminates and single-sided and double-sided copper-clad laminates was not the same. Furthermore, the glass-fiber fracture, the glass-fiber stripping from the substrate and matrix cracking were characterized by the amplitude, count, rise time, duration time, energy of AE signals during the three-point bending.

1. Introduction

Glass-fiber reinforced laminates and copper-clad laminates were widely used in automobile, railway, aerospace, electronics industry, ship, decorative buildings, home furnishings, building materials bathroom and sanitation engineering, the ease with which they may be formed into complex shapes, and also their high specific strength and stiffness [1–4]. In particular, copper-clad laminates was widely used in the electronics industry, as the electronic components of the carrier and electrical signal connection, which directly affected the reliability of control system. Every year, due to such an accident, causing huge economic losses.

Therefore, many researchers were focused on the fatigue behavior [5], mechanical behavior [6,7], the interface property [8–10], the defects of glass-fiber reinforced laminates and copper-clad laminates [11,12]. At the same time, finite element analysis (FEA) was applied to simulate the deformation [13], damage [14], damage evolution [15] and the effects of fiber volume fractions [16] of glass-fiber reinforced laminates. Moreover, some researchers studied on the damage initiation [17], damage evolution, the failure [18,19] and the delamination fracture toughness [20] of glass-fiber reinforced with acoustic emission (AE).

Although, in the past decade, a large number of studies on the theoretical models, simulations and experiments on glass-fiber reinforced laminates and copper-clad laminates have been conducted. However, compared with the studies on the damage of glass-fiber, our understanding of the copper film influence on the failure mechanism of copper-clad laminates under three-point bending (TPB) was far from complete. Researches on the microscopic morphology of copper-clad laminates by using *in situ* microscope were rarely during the three-point bending (TPB).

Therefore, in this paper, the damage evolution of microscopic morphology of the copper-clad laminates side surface was *in situ* recorded during the TPB. Simultaneously, AE was used to characterize the glass-fiber breakage, fiber/matrix debonding and matrix cracking of glass-fiber reinforced laminates. Moreover, finite element analysis was applied to simulate the stress distribution on the specimen of glass-fiber reinforced laminates and copper-clad laminates during the TPB

* Corresponding author.
E-mail address: hwzhao@jlu.edu.cn (H. Zhao).

https://doi.org/10.1016/j.ijadhadh.2018.05.006
Accepted 5 May 2018
Available online 16 May 2018
0143-7496/

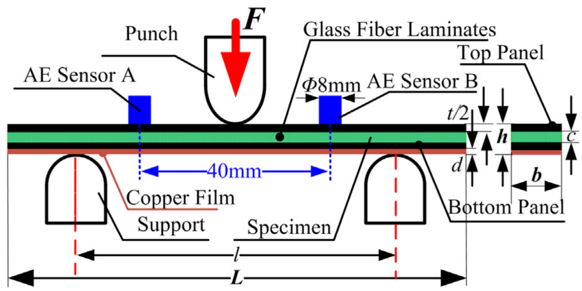

Fig. 1. The theoretical model of TPB test.

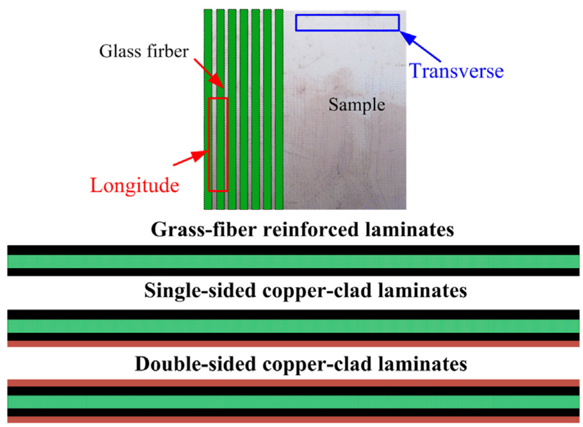

Fig. 2. The type of specimens and sampling in the direction.

bending. The copper film can dramatically influence the failure mechanism of glass-fiber reinforced laminates.

2. Experiment

2.1. Theory of experiment

In this experiment, the specimens were tested under three-point bending as shown in Fig. 1.

In or order to simplify the theoretical model, the glass-fiber reinforced laminates and copper-clad laminates were considered as sandwich beam. During the three-point bending of the sandwich beam,

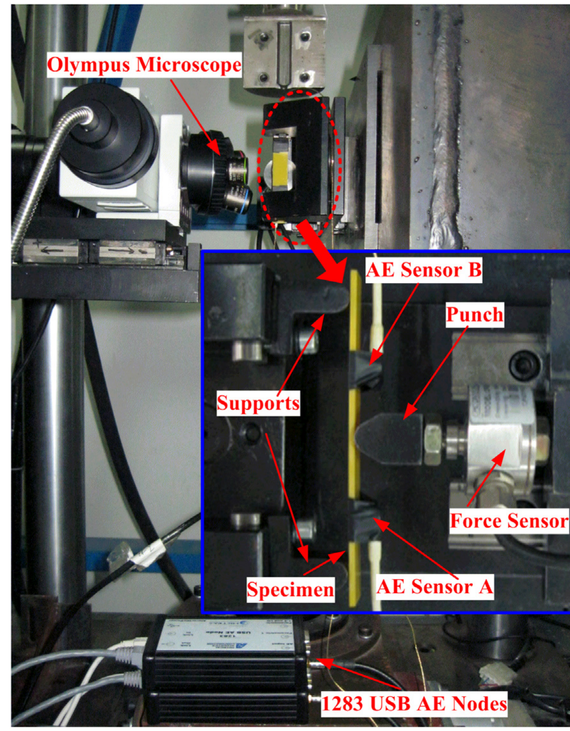

Fig. 3. The TPB test system in this experiment.

Table 2
AE control parameter settings in this experiment.

PDT	HDT	HLT	Analog filter	Threshold	Sample rate
30 μs	600 μs	1000 μs	200k-1 MHz	35 dB	5 MHz

the relationship between load F and deflection f can be expressed as follows [21]:

$$f = \frac{Fl^3}{48(EI)_{eq}} + \frac{Fl}{4(AG)_{eq}} \quad (1)$$

$$(EI)_{eq} = \frac{E_f bt(c+t)^2}{2} + \frac{E_f bt^3}{6} + \frac{E_c bc^3}{12} \quad (2)$$

Table 1
Specimen type, the thickness of copper film, sampling direction and dimension size.

Specimen type	Copper thickness	Sampling direction	Dimension (L (mm) × b (mm) × h (mm))		
			1	2	3
No copper	d = 0 μm	Longitude	100.08 × 14.11 × 1.48	99.94 × 14.05 × 1.51	100.05 × 13.98 × 1.49
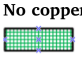		Transverse	100.12 × 14.13 × 1.49	100.10 × 13.97 × 1.50	100.13 × 14.14 × 1.51
Single-sided	d = 10 μm	Longitude	100.06 × 14.12 × 1.51	100.04 × 14.04 × 1.52	99.97 × 13.98 × 1.54
		Transverse	99.96 × 13.98 × 1.53	100.07 × 14.07 × 1.52	100.13 × 14.14 × 1.51
	d = 17 μm	Longitude	100.01 × 14.06 × 1.52	99.98 × 14.02 × 1.53	100.06 × 13.98 × 1.51
		Transverse	100.12 × 14.13 × 1.50	100.10 × 13.97 × 1.52	100.13 × 14.14 × 1.52
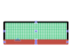	d = 35 μm	Longitude	100.08 × 14.11 × 1.54	99.94 × 14.05 × 1.55	100.11 × 13.98 × 1.52
		Transverse	100.12 × 14.13 × 1.52	100.10 × 13.97 × 1.53	100.13 × 14.14 × 1.54
	d = 50 μm	Longitude	100.05 × 14.02 × 1.55	100.10 × 14.15 × 1.56	100.13 × 14.08 × 1.57
		Transverse	100.14 × 14.06 × 1.54	100.12 × 13.98 × 1.55	100.08 × 14.04 × 1.56
Double-sided	2d = 20 μm	Longitude	100.07 × 14.12 × 1.52	99.98 × 14.05 × 1.51	100.10 × 13.99 × 1.52
		Transverse	100.02 × 14.07 × 1.53	100.12 × 13.99 × 1.51	100.03 × 14.04 × 1.54
	2d = 34 μm	Longitude	100.10 × 14.10 × 1.53	99.98 × 14.02 × 1.54	100.12 × 13.96 × 1.52
		Transverse	100.13 × 14.06 × 1.53	100.08 × 13.98 × 1.52	100.10 × 14.11 × 1.54
	2d = 70 μm	Longitude	100.08 × 14.12 × 1.58	99.97 × 14.03 × 1.57	100.10 × 13.97 × 1.59
		Transverse	100.07 × 14.10 × 1.56	100.13 × 13.98 × 1.55	100.07 × 14.08 × 1.58
	2d = 100 μm	Longitude	100.04 × 14.11 × 1.59	100.04 × 14.01 × 1.61	100.06 × 14.08 × 1.60
		Transverse	99.94 × 14.10 × 1.61	100.05 × 14.07 × 1.62	100.12 × 14.10 × 1.58